Tensile/flexural fracture behavior of composite specimens combining SHCC and concrete

T. Mizuta & K. Rokugo
Department of Civil Engineering, Gifu University, Japan

T. Inaguma
Central Japan Railway Consultants Co., Ltd, Japan

ABSTRACT: Tensile and flexural fracture behavior of composite specimens made of SHCC and normal concrete (NC) was investigated. Uniaxial tension tests on these materials were successfully carried out without breaking the enlarged ends of dumbbell specimens by a method in which their shoulders are engaged in locks and subjected to tensile loading. Composite specimens under bending action having NC on the tension side underwent early cracking in NC, resulting in a lower load-bearing capacity of specimens and smaller deformation of SHCC. In composite specimens having SHCC on the outside of NC, cracks in NC under tensile and bending action were rendered fine and multiple ahead in the outer layer of SHCC.

1 INTRODUCTION

Strain-hardening fiber-reinforced cement-based composites (SHCC) (Naaman & Reinhardt 1995, Li 1993, Kunieda & Rokugo 2006) are a highly ductile cementitious material showing multiple-cracking characteristics and pseudo-strain-hardening characteristics under tensile and bending forces. When applied to newly built structural members, SHCC may be used as part of composite members with normal concrete (NC), which shows brittle fracture characteristics. It may also be used for surface repair of concrete structures having cracks to control the surface crack widths.

This study aims to experimentally elucidate the tensile/flexural fracture behavior of composite specimens combining SHCC and NC focusing on the load, deformation, and cracking.

2 OUTLINE OF EXPERIMENT

2.1 *Materials*

Table 1 gives the mix proportions of SHCC and NC. High-early-strength portland cement was used as the cement for both. SHCC included No. 7 silica sand as fine aggregate and polyethylene fibers 0.012 mm in diameter and 12 mm in length at a fiber ratio of 1.5% by volume. Crushed stone with a maximum size of 15 mm was used as coarse aggregate for NC.

Table 1. Mix proportions of SHCC and NC.

Types of material	Cement (kg/m^3)	Water/Cement ratio (%)	PE fiver (vol%)
SHCC	1264	30	1.5
NC	331	55	-

2.2 *Uniaxial tension testing*

2.2.1 *Tension specimens*

The geometry and types of tension specimens are shown in Fig. 1 (a) and Table 2, respectively. The specimens were of a dumbbell type measuring 400 mm in length, 100 mm in depth, and 100 and 60 mm in width at the enlarged ends and narrowed center, respectively. For composite specimens with NC sandwiched between two SHCC layers (“SNS” specimens), an SHCC layer was placed to a depth of 25 mm, followed by a NC layer of 50 mm and then another SHCC layer of 25 mm. Each layer was placed within 2 hours after placing the previous layer. Composite specimens with SHCC sandwiched between two NC layers (“NSN” specimens) were also fabricated similarly. Two specimens were prepared for each set of conditions due to limitations of molds.

2.2.2 *Tension test procedure*

Figure 2 shows the uniaxial tension test setup. The enlarged ends of each specimen were engaged in

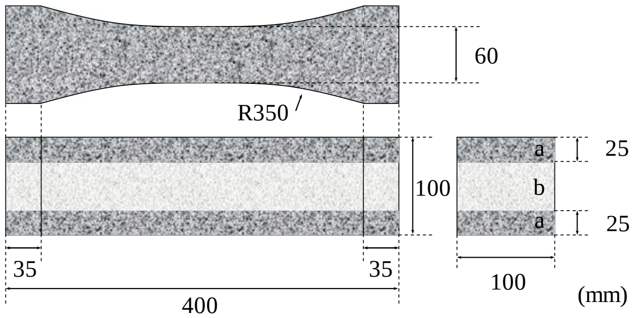

(a) Tension specimens

(b) Flexure specimens

Figure 1. Specimen geometry.

Table 2. Tension specimens.

Series	Layer	Types of material
SNS	a	SHCC
	b	NC
NSN	a	NC
	b	SHCC
SHCC	a	SHCC
	b	
NC	a	NC
	b	


Figure 2. Uniaxial tension test setup.

steel locks. Both the clamps on the right and left sides of each lock were fixed with bolts to prevent them from opening apart during testing. Stiff-mix gypsum that begins to harden in around 10 min was thinly inserted between the clamps and specimens of NSN, SNS, and homogeneous NC to alleviate localized stress concentration.

Loading was applied using a center hole-type hydraulic jack and monitored with a load cell. The displacement was detected using an accurate displacement transducer attached to the central part of the specimen with respect to a gage length of 100 mm. The lower end of each specimen was fixed while the upper end was roller-supported. The test ages ranged from 18 to 25 days.

2.3 *Bending testing*

2.3.1 *Flexure specimens*

The geometry and types of flexure specimens used in this study are shown in Fig. 1 (b) and Table 3, respectively. These beam specimens measured 100 mm in width, 100 mm in depth, and 400 mm in length. For "SC#" composite specimens, NC was placed to a depth of 0, 10, 20, 30 or 40 mm from the tension side, followed by SHCC. For "CS#" composite specimens, SHCC was conversely placed in the tension side ("#" represents the depth of the material on the tension side). Note that the cases of 0 mm are homogeneous specimens. Homogeneous specimens with a depth of 60 to 90 mm were also fabricated in addition. Basically two specimens were fabricated for each set of conditions.

2.3.2 *Bending test procedure*

Bending tests were conducted by third-point loading at test ages of 18 to 25 days similarly to uniaxial tension tests. The loads were monitored with a load cell, while detecting the displacement using accurate displacement transducers placed at the support points and load points.

2.4 *Crack observation*

In addition to visual observation, the images of cracks were scanned into a PC using a microscope of 50 magnifications (VH-5000 manufactured by Keyence Corporation).

Table.3 Flexure specimens.

Series	Layer	Types of material	Depth (mm)				
SC#	a	SHCC	100	90	80	70	60
	b	NC	0	10	20	30	40
CS#	a	NC	100	90	80	70	60
	b	SHCC	0	10	20	30	40

#：Represents depth of material on tension side

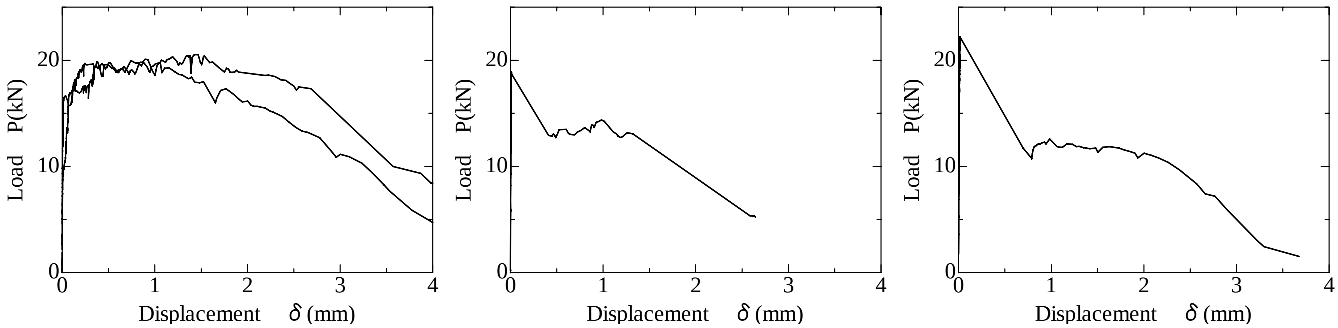

(a) SHCC (b) SNS (c) NSN

Figure 3. Load-displacement relationships obtained from uniaxial tension tests.

3 TEST RESULTS

3.1 *Uniaxial tension testing*

3.1.1 *Fracture location and peak load*

The fracture (rupture of NC and crack widening in SHCC) was localized to the narrowed center (60 mm in width) of each specimen. In other words, uniaxial tension tests on SHCC and NC were successfully carried out without breaking the enlarged ends of dumbbell specimens by engaging their shoulders in the locks and applying tensile forces.

The peak loads obtained from the uniaxial tension tests are given in Table 4. The peak loads of composite specimens made of SHCC and NC were intermediate values between those singly made of SHCC and NC. In other words, the tensile capacities of composite specimens were the sum of those of homogeneous SHCC and NC specimens.

Table 4. Peak loads obtained from uniaxial tension tests.

Series	Peak loads (kN)		Average (kN)
SNS	23.0	18.9	20.9
NSN	22.2	20.1	21.1
SHCC	19.8	20.5	20.2
NC	26.5	19.8	23.1

3.1.2 *Load-displacement relationship*

Figure 3 shows the load-displacement relationships obtained from the uniaxial tension tests. Homogeneous SHCC specimens showed clear pseudo-strain-hardening behavior in which the load increased after the first cracking. In regard to composite specimens made of SHCC and NC at a cross-sectional area ratio of 50:50, cracking occurred in NC at the point of the peak load. The load then rapidly decreased, ending up in brittle failure. This can be attributed to the fact that the tensile force borne by NC cannot be carried only by the load increment of SHCC owing to its post-cracking strain-hardening.

When a combination of NC and SHCC is used for members subjected to tensile action, it is generally expected to include steel reinforcement. In such a case, it is necessary to adequately plan the bar arrangement so that the tensile forces are stably borne by such members after crack onset in NC in a similar manner as the requirement for the minimum reinforcement ratio of reinforced concrete members.

One each of the two specimens of NSN and SNS underwent rapid rupture, with the displacement being out of control after the peak load, but the displacement of the other ones was measurable in the course. The maximum load of composite specimens, which is borne by SHCC after the peak load owing to the bridging of fibers, was found to be 1.2 times the value expected for homogeneous SHCC specimens (half the load of specimens with a depth of 100 mm). This is presumably because the ultimate fracture zone of SHCC is limited to the location of large cracks in NC and because not only SHCC but also crackless portions of NC bear part of the tensile forces.

No marked difference was observed between the deformations of composite specimens after the peak load that were measurable and those of homogeneous SHCC specimens. However, this requires further investigation due to the small numbers of specimens.

3.1.3 *Cracking*

In the SNS specimen whose displacement after crack onset in NC was under control, the cracking in the outer SHCC layers was consisted of multiple fine cracks even after cracking occurred in the inner NC layer. Cracks in the central SHCC layer in the NSN specimen were similarly fine and multiple.

Figures 4 and 5 show the photographs of cracking on the side surfaces of specimens observed after uniaxial tension testing. Whereas localized wide cracks are found in the NC layer, these are arrested into multiple fine cracks in the SHCC layer. The cracking regions in SHCC were limited by cracking in NC.

3.2 *Bending testing*

3.2.1 *Composite ratio and peak load*

(a) Photograph (b) Circle (1) (c) Circle (2)

Figure 4. Photographs of cracking on side surfaces of specimens (SNS).

(a) Photograph (b) Circle (1) (c) Circle (2)

Figure 5. Photographs of cracking on side surfaces of specimens (NSN).

Figure 6 shows the relationship between the depth of NC or SHCC from the tension side and the peak load of composite specimens. The results of homogeneous NC and SHCC specimens with a depth of 60 to 90 mm are superimposed as broken lines. The solid line in Fig. 6 (a) represents the expected peak load neglecting NC on the tension side (proportional to the square of the depth of the SHCC layer).

The peak load of composite specimens with NC on the tension side is significantly lower than the level of the broken line and close to the solid line, which neglects NC. This can be attributed to large cracking in NC at an early stage.

On the other hand, the peak load of composite specimens with SHCC on the tension side is similar to the level of the broken line. It is therefore inferred that both SHCC and NC contribute to the resistance to the bending action, thanks to the large deformability of SHCC.

3.2.2 *Load-displacement curve*

The load-displacement curves obtained from the bending tests are shown in Figs. 7 and 8. The displacement (e.g., those corresponding to the point of the maximum load after the effect of fibers has been developed) of specimens having the NC layer on the tension side is as low as 1/2 to 1/3 of that of homogeneous SHCC specimens with the same SHCC depth (e.g., SH80). In other words, placing a brittle layer of NC on the outside of highly ductile SHCC restricts the deformability of SHCC. In this light, care should be exercised when using SHCC in combination with normal concrete and asphalt concrete.

On the other hand, SHCC on the tension side bears the load and deforms after cracking occurs in NC, and the displacement increases as the depth of SHCC increases. The load-displacement curve of specimens having SHCC to a depth of 40 mm on the tension side is close to that of homogenous SHCC specimens. Placing SHCC on the tension side of brittle NC subjected to bending action thus improves the load-bearing capacity and deformability of such composite specimens.

3.2.3 *Cracking*

The state of cracking after bending tests is shown in Figs. 9 and 10. Figures 7 and 8 show the average areas under the load-displacement curves of composite specimens up to the point of the maximum load after the effect of fibers has been developed. Figure 10 clearly shows that cracks that occurred in NC propagate into SHCC, turning into multiple fine cracks. Specimens with a larger area under the load-displacement curve tend to have larger cracking regions on their side surfaces with a larger number of cracks. The authors intend to continue investigation focusing on cracking regions and the number of cracks.

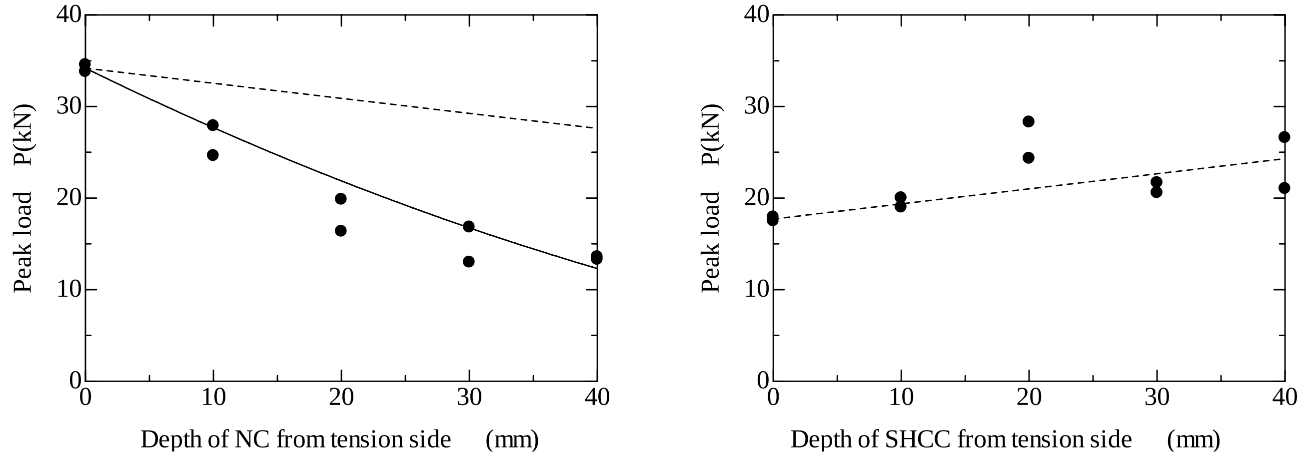

(a) Series SC# (b) Series CS#

Figure 6. Relationship between depth of NC or SHCC from tension side and peak load of composite specimens.

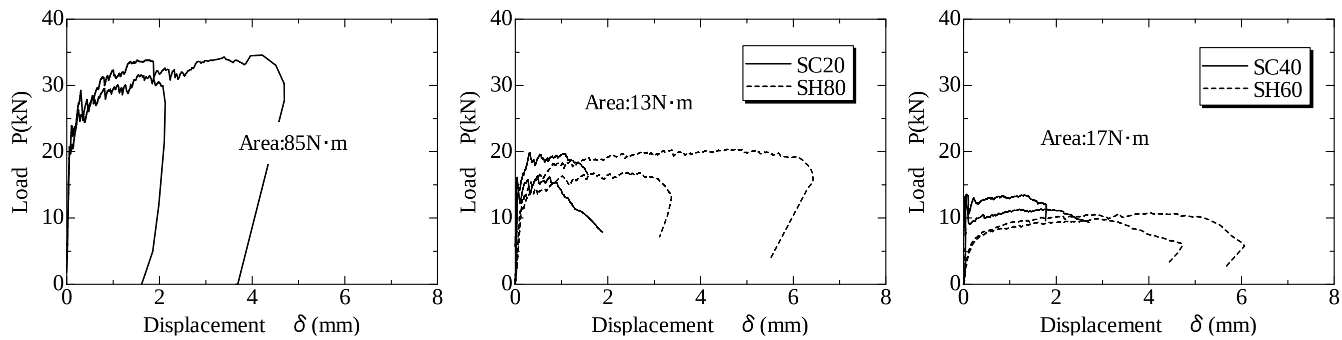

(a) SC0 (b) SC20 (c) SC40

Figure 7. Load-displacement curves obtained from bending tests (SC#).

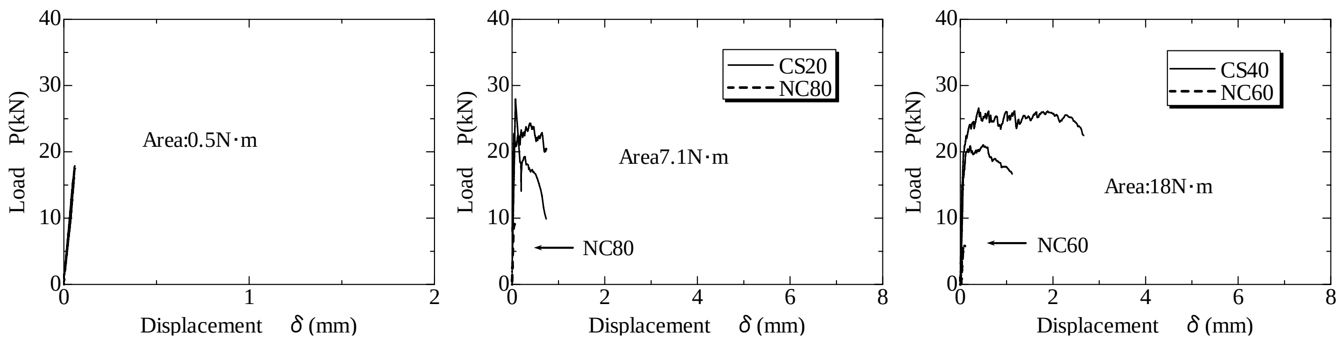

(a) CS0 (b) CS20 (c) CS40

Figure 8. Load-displacement curves obtained from bending tests (CS#).

4 CONCLUSIONS

The results of this study are summarized as follows:

- Uniaxial tension tests on SHCC and NC were successfully carried out by employing a method in which the shoulders of dumbbell-shaped tension specimens are engaged in locks and subjected to tensile forces.
- Uniaxial tension tests on composite specimens having a cross-sectional area ratio of SHCC to NC of 50:50 led to cracking in NC at the peak load, followed by rapid reductions in the load, ending up in brittle failure.
- When subjected to bending action, composite specimens having SHCC on the tension side and NC on the inside showed increased load and deformation. However, specimens conversely having NC on the tension side not only showed early cracking in NC, which reduced their load-bearing capacity, but also restricted the deformation of SHCC.

– When specimens having a SHCC layer on the outside of a NC layer were subjected to tensile and flexural action, newly occurring cracks in NC were arrested into multiple fine cracks in the outer SHCC layer.

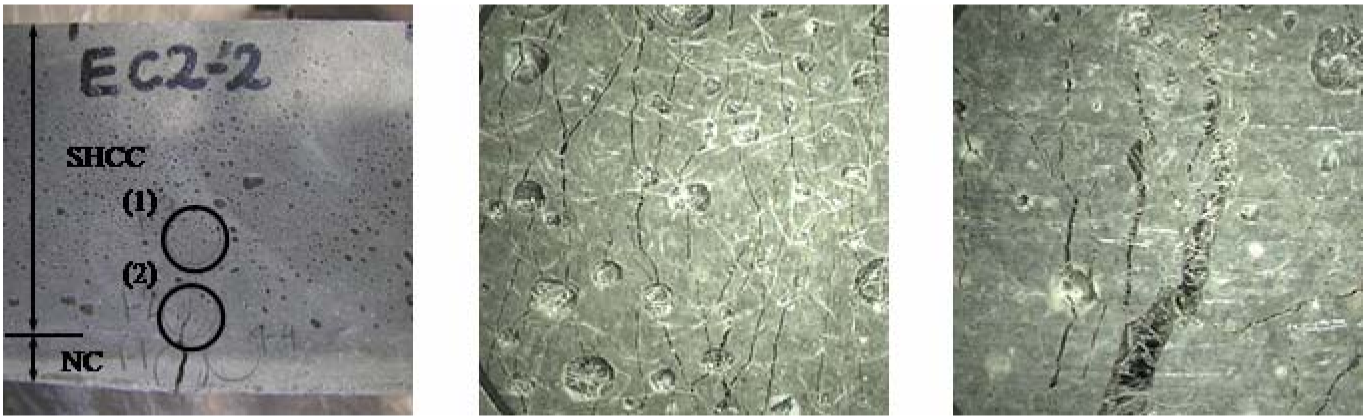

(a) Photograph (b) Circle (1) (c) Circle (2)

Figure 9. Photographs of cracking on side surfaces of specimens (SC20).

(a) Photograph (b) Circle (1) (c) Circle (2)

Figure 10. Photographs of cracking on side surfaces of specimens (CS20).

REFERENCES

Naaman, A.E. & ReH.W inhardt. (eds.) 1995. *High Performance Fiber Reinforced Cement Composites 2 (HPFRCC 2), RILEM Proceedings 31*. London, E&FN Spon.

Li, V.C. 1993. From Micromechanics to Structural Engineering -The Design of Cementitious Composites for Civil Engineering Applications. *J. Struct. Mech.Earthquake Eng.*, JSCE, 10 (2): 37-48.

Kunieda, M. & Rokugo, K. 2006. Recent Progress on HPFRCC in Japan - Required Performance and Applications -, *Journal of Advanced Concrete Technology,* JCI, 4(1): 19-33.